
Reference-Guided Identity Preserving Face Restoration

Mo Zhou^{1,2*} Keren Ye¹ Viraj Shah¹ Kangfu Mei¹ Mauricio Delbracio¹
Peyman Milanfar¹ Vishal M. Patel² Hossein Talebi¹
¹Google ²Johns Hopkins University

Abstract

Preserving face identity is a critical yet persistent challenge in diffusion-based image restoration. While reference faces offer a path forward, existing reference-based methods often fail to fully exploit their potential. This paper introduces a novel approach that maximizes reference face utility for improved face restoration and identity preservation. Our method makes three key contributions: 1) Composite Context, a comprehensive representation that fuses multi-level (high- and low-level) information from the reference face, offering richer guidance than prior singular representations. 2) Hard Example Identity Loss, a novel loss function that leverages the reference face to address the identity learning inefficiencies found in the existing identity loss. 3) A training-free method to adapt the model to multi-reference inputs during inference. The proposed method demonstrably restores high-quality faces and achieves state-of-the-art identity preserving restoration on benchmarks such as FFHQ-Ref and CelebA-Ref-Test, consistently outperforming previous work.

1 Introduction

Recently, image restoration [1, 2, 3, 4, 5, 6] has seen significant improvements along with the rise of diffusion models [7, 8], particularly in terms of generated image quality [9, 10]. However, the state-of-the-art restoration methods, including the face-specific ones [11, 4, 12, 13], still suffer from unsatisfactory identity preservation when processing facial imagery. This limitation can substantially degrade the user experience, given the human perceptual acuity for subtle variations in facial features.

In some real-world applications, such as digital albums, when restoring a low-quality face image, it is possible to leverage other high-quality face images from the same person as references to better preserve the identity and appearance. Consequently, many reference-based face restoration methods [12, 13, 14, 15] have been proposed. These efforts involve designing novel architectures for reference face conditioning [13, 12], formulating new loss functions for identity preservation and image quality [12, 14], and curating specialized reference-based face restoration datasets [12, 15]. Nevertheless, the existing methods do not fully exploit the potential of reference faces, and hence there is room for improvement in both identity preservation and image quality.

In this paper, to more effectively utilize the reference face images and further enhance the performance of reference-based face restoration, we propose two independent modules that exploit the reference face in two different aspects: representation and supervision.

First, we propose Composite Context, a comprehensive representation for the reference face. It consists of multiple pre-trained face representations that focus on different information in the reference face from high-level to low-level. Specifically, it includes identity embedding [16] as high-level identity information; and general face representation [17] comprising both high-level semantic information and low-level face information. These comprehensive and multi-level representations

*Work done during internship at Google LLC.

can exploit the reference face images better than previous work that only uses a single type of representation [13, 18, 12], capturing only partial information which is insufficient. For example, the face embedding [19, 16] only contains identity information, while other potentially useful details like the visual appearance of the reference face are not encoded in face embedding at all.

Second, we propose Hard Example Identity Loss. It is a simple yet effective extension of the existing identity loss [12], motivated by the empirical observation that traditional identity loss functions suffer from learning inefficiencies – a well-documented issue in the metric learning literature [19, 20, 21]. In particular, the ground-truth faces are not hard enough (see “Triplet Selection” in [19] for the meaning of “hard example”), which makes the identity loss magnitude very small after a short period of training. By simply incorporating a hard sample, namely the reference face, into the identity loss, the learning inefficiency problem can be effectively addressed, and hence leads to a significant performance improvement. In contrast, all previous works [18, 12, 14] overlooked this issue.

Apart from the representation and supervision aspects, while our method is designed to take a single reference face image, it can be extended to support multiple reference face images through a simple method based on classifier-free guidance [22] at the inference stage, which requires no extra training.

Our qualitative and quantitative experimental results on the FFHQ-Ref [12] and CelebA-Ref-Test [12] datasets demonstrate the effectiveness of our method. Though simple, our method effectively and consistently outperforms the previous methods in face identity preservation.

Contributions. Our contributions are threefold regarding reference-based face image restoration:

- We propose “Composite Context”, a comprehensive face representation that involves multi-level information extracted from the reference face.
- We propose “Hard Example Identity Loss”, an extension to the existing identity loss that incorporates the reference face for improved learning efficiency and identity preservation.
- We extend the proposed model to flexibly support multi-reference faces at the inference stage in a training-free manner, even though the model only uses a single reference face during training.

2 Related Work

Image Restoration. As diffusion models [7, 9, 8, 23, 24, 25] gain popularity in image generation, LDM [9] has recently become a popular backbone for general image restoration [2, 4, 3, 6, 5, 26]. However, humans are perceptually highly sensitive to subtle differences in face images, general image restoration techniques typically perform poorly, especially in terms of identity preservation and maintaining face image realism. In this case, face-specific restoration models are preferred.

No-reference Face Restoration. When there is no reference face, generative models can be used to hallucinate details while restoring a degraded facial image [11, 4, 18, 27, 28, 29, 30, 31]. CodeFormer [11] presents a Transformer [32] to model the global composition and context of the low-quality faces for code prediction, enabling the generation of natural faces that closely approximate the target faces. DiffBIR [4] presents a two-stage pipeline for blind face restoration, involving the degradation removal stage and information regeneration stage. OSDFace [18] proposes a visual representation embedder to capture information from the low-quality input face and incorporate the face identity loss for identity preservation. A common challenge in no-reference face restoration is identity preservation since no additional information is provided.

Reference-based Face Restoration. High-quality reference face images, when available, can help identity preservation when restoring a low-quality face of the same person [33, 12, 13, 14, 15, 34]. DMDNet [15] proposes a dual memory dictionary for both general and identity-specific features for blind face restoration. RestorerID [13] presents a Face ID Adapter and incorporates the identity embedding of the reference face as a tuning-free face restoration method. InstantRestore [14] leverages a one-step diffusion model, and proposes a landmark attention loss to enhance identity preservation. RefLDM [12] incorporates the CacheKV mechanism and a timestep-scaled identity loss into an LDM [9] to effectively utilize multiple reference faces for face restoration. Personalization methods [34, 35] utilizes reference faces with the goal of customizing the model for individual users.

Key Differences. This paper focuses on reference-based face restoration. The most related works to this paper are RefLDM [12], RestorerID [13], and InstantRestore [14]. The key differences between our method and the previous methods are: (1) The previous methods only use a single

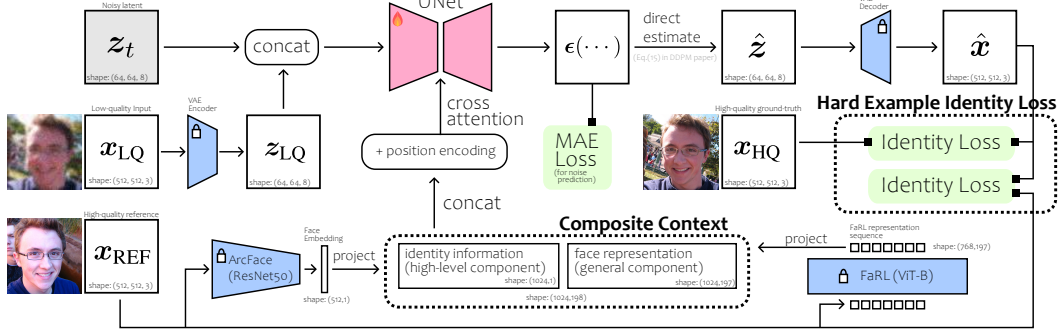


Figure 1: Overview of our proposed method. The Composite Context and Hard Example Identity Loss are designed for fully exploiting the reference face and hence boost identity preservation. The z_t is the noisy latent, x_{LQ} is the low-quality face image input (z_{LQ} is its corresponding VAE latent), x_{REF} is the high-quality reference face, x_{HQ} is the high-quality ground-truth face image, \hat{z} is the direct estimate of the denoised result (*i.e.*, Eq. (15) in DDPM [7]), and \hat{x} is the VAE decoded direct estimate. All pre-trained modules are frozen. The UNet [37] and projection matrices for Composite Context are trained. The total loss includes the MAE loss and the Hard Example Identity Loss.

representation for the reference face, which only covers partial information of the reference and does not maximize the utilization of the reference. In contrast, our Composite Context combines multi-level face-specific representations to comprehensively exploit the information in the reference face. The Composite Context conceptually resembles [26, 36] which employ multiple modalities to aid image restoration, and [10] which concatenates two text representations for text-to-image synthesis. (2) While many related works [12, 18, 14] incorporate the identity loss, a notable learning inefficiency issue where the loss value plateaus at a tiny value (indicates learning inefficiency in the context of metric learning [20, 21, 19]) has been overlooked. We propose Hard Example Identity Loss to incorporate “hard examples” to address this issue. (3) Some existing methods support only one reference face [13]. Some others support multiple [12], but also require multiple reference face images during training. It is noted that requiring more than one reference face makes training data collection difficult. In contrast, even if our method only uses one reference face during training, our model can be adapted to support multiple reference faces during inference in a training-free manner.

3 Our Approach

Given a low-quality (LQ) face image x_{LQ} , and a high-quality (HQ) reference face image x_{REF} from the same person, we aim to restore the LQ image while preserving the person identity by leveraging the reference face. The resulting image should be close to the ground truth HQ image x_{HQ} in terms of both identity similarity and perceptual similarity.

To this end, we adopt a general LDM [9] backbone pretrained for text-to-image synthesis. Following the previous works [9, 12], we incorporate the LQ input image x_{LQ} by conditioning the diffusion model on its corresponding VAE latent z_{LQ} through concatenating it to the noise latent z_t . In this way, the model $\epsilon(z_t, z_{LQ}, t)$ can serve as a fundamental face image restoration model.

In order to comprehensively leverage the reference face for better identity preservation, we propose two independent modules: Composite Context (CC) and Hard Example Identity Loss (HID), which will be detailed in Section. 3.1 and Section. 3.2 below. In brief, the Composite Context is a comprehensive representation c from the reference face x_{REF} . It is used as a condition for $\epsilon(z_t, z_{LQ}, c, t)$ through cross-attention mechanism [9]. Then, the Hard Identity Loss \mathcal{L}_{HID} will take advantage of the reference face to enhance identity preservation. See Figure 1 for the overview of our method.

3.1 Composite Context for Comprehensive Reference Face Representation

Different from no-reference face restoration methods, reference-based face restoration [12, 13, 14] assumes that a high-quality reference face from the same person is available. To thoroughly leverage this advantage, we propose Composite Context, a comprehensive representation of the reference face image that covers multi-level information from the reference face, including high-level semantic

information (such as person identity) and low-level appearance information (such as skin texture). Unlike previous works [18, 12, 13, 14] that only leverage partial information from the reference face through a single representation, Composite Context allows the model to comprehensively leverage the reference face at different levels. Therefore, Composite Context may benefit identity preservation.

Given a reference face image x_{REF} which belongs to the same identity as x_{LQ} , we can leverage a collection of pre-trained face representation models for various purposes to extract the respective representations, and combine them together as a vector sequence. In particular, Composite Context consists of the following multi-level components:

- **High-level features:** ArcFace [16] embedding representing person identity. ArcFace is a face recognition model which enforces an angular margin loss in its embedding space. We assume that $\phi_{\text{H}}(\cdot)$ is the pre-trained ArcFace model in the standard ResNet50 [38] architecture, and \mathbf{W}_{H} is a projection matrix from the dimensionality of face embedding to the dimension of UNet cross-attention. The projected embedding $\mathbf{W}_{\text{H}}\phi_{\text{H}}(x_{\text{REF}})$ is the first part of the Composite Context.
- **General features:** FaRL [17] representation representing various high-level semantic (*e.g.*, face attributes) and low-level information (*e.g.*, visual appearance) of the reference face. FaRL is a general face representation model learned in a visual-linguistic manner, with image-text contrastive learning and masked image modeling simultaneously [17]. We assume that $\phi_{\text{G}}(\cdot)$ is a pre-trained FaRL model (ViT-B [39] architecture), and \mathbf{W}_{G} is the projection matrix to the dimension of UNet cross-attention. We use the whole output sequence (197 tokens) from FaRL to maximize reference face utility. The projected sequence $\mathbf{W}_{\text{G}}\phi_{\text{G}}(x_{\text{REF}})$ is the second part of the Composite Context.

After obtaining those different representations from the reference face x_{REF} , they are concatenated, and added with the standard sinusoidal positional encoding [32] as the Composite Context:

$$c = \text{Concat}[\mathbf{W}_{\text{H}}\phi_{\text{H}}(x_{\text{REF}}), \mathbf{W}_{\text{G}}\phi_{\text{G}}(x_{\text{REF}})] + e_{\text{position}}, \quad (1)$$

where e_{position} denotes sinusoidal positional encoding [32]. Since all the Composite Context components are from pre-trained models, the sequence length is fixed at $1 + 197 = 198$ for any reference face. Finally, the Composite Context c is incorporated into the model through the cross-attention conditioning mechanism [9] as $\varepsilon(z_t, z_{\text{LQ}}, c, t)$. See Figure 1 for the overall diagram.

3.2 Hard Example Identity Loss for Improved Learning Efficiency

One of the goals of face restoration is to preserve the identity, which means the restored face should match the identity of the HQ image. To achieve this, many recent works [12, 18, 14] incorporate the identity loss, which is based on a pre-trained face embedding model [16, 19] such as ArcFace [16]. In particular, RefLDM [12] presents a timestep-scaled identity loss \mathcal{L}_{ID} as:

$$\mathcal{L}_{\text{ID}}(x_{\text{HQ}}, \hat{x}) = \sqrt{\alpha_t} \cdot (1 - \cos(\phi_{\text{H}}(x_{\text{HQ}}), \phi_{\text{H}}(\hat{x}))), \quad (2)$$

where ϕ_{H} denotes the face embedding model [16], the notation $\sqrt{\alpha_t}$ is inherited from DDPM [7], and \hat{x} is the direct estimate of x_0 at time step t , *i.e.*, Eq. (15) in DDPM [7]. The time-step scaling factor $\sqrt{\alpha_t}$ mitigates the out-of-domain behavior of the identity loss at a very noisy step t , and emphasizes identity preservation at less noisy steps. However, a learning inefficiency issue is overlooked.

During experiments, we observe that the identity loss in Eq. (2) decreases quickly and plateaus at a very small magnitude, as shown by the blue curve in Figure 2. In the metric learning literature [19, 20, 21, 40, 41], there is a similar phenomenon where the loss value is small when the training samples are not hard enough (see ‘‘Triplet Selection’’ in [19]), which usually leads to poor generalization. Their countermeasure is to mine some hard examples [19] that can trigger a larger loss value so the model performance can be drastically influenced [21]. Inspired by such solution to the learning inefficiency issue, we propose to leverage the reference face x_{REF} as a hard example in addition to x_{HQ} . Based on this, we design a simple extension to the identity loss \mathcal{L}_{ID} as the ‘‘Hard Example Identity Loss’’ incorporating the hard example, namely the reference face.

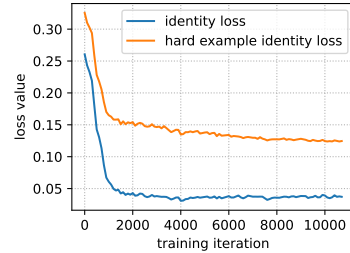


Figure 2: Loss curves of \mathcal{L}_{ID} and \mathcal{L}_{HID} during the training process. The curves are truncated to the beginning part of the training process.

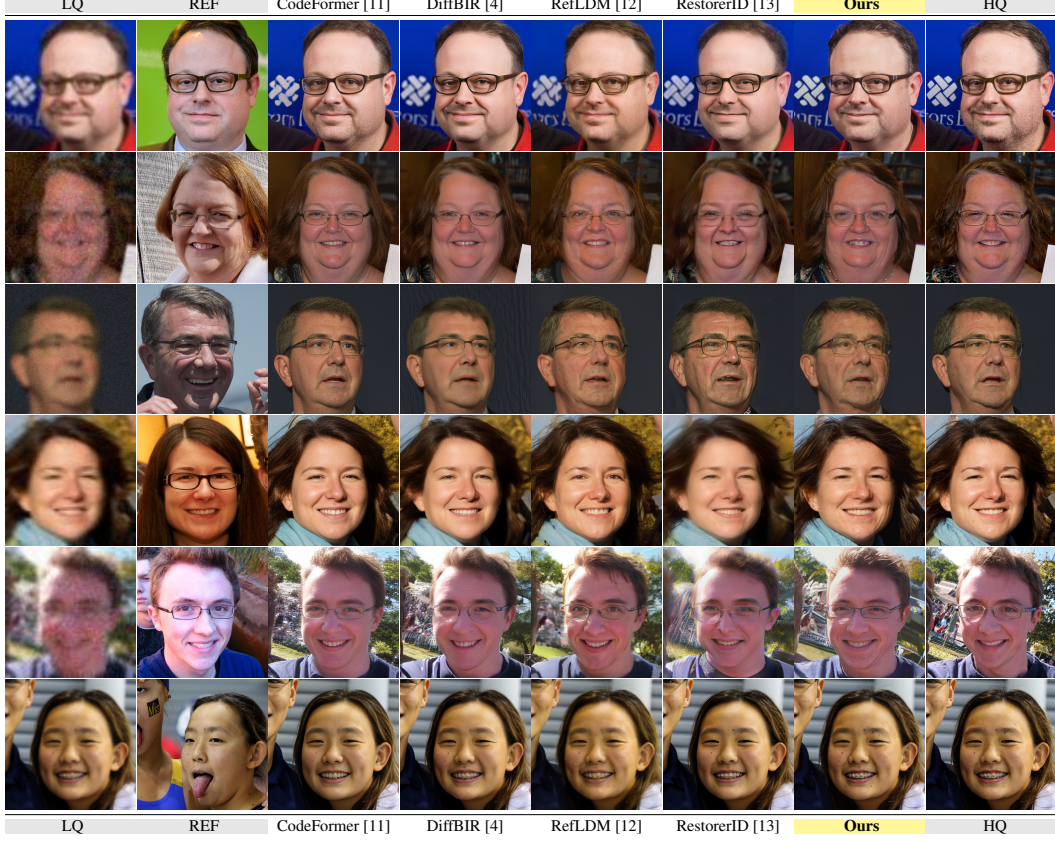


Figure 3: Qualitative comparison with other state-of-the-art face restoration methods on FFHQ-Ref Moderate [12] test set. The “REF” column is the reference face. Please zoom in for the face details. For instance, the black moles are well-preserved in our result on the sixth row.

Let λ be a hyper-parameter for balancing the influence of x_{HQ} and x_{REF} during training. Formally, the Hard Example Identity Loss \mathcal{L}_{HID} is also based on the direct estimate \hat{x} , and is defined as:

$$\mathcal{L}_{\text{HID}}(x_{\text{HQ}}, x_{\text{REF}}, \hat{x}) = (1 - \lambda)\mathcal{L}_{\text{ID}}(x_{\text{HQ}}, \hat{x}) + \lambda\mathcal{L}_{\text{ID}}(x_{\text{REF}}, \hat{x}). \quad (3)$$

As shown by the orange curve in Figure 2, our Hard Example Identity Loss will no longer plateau at a very small value because a “harder” example is introduced, and hence will alleviate the learning inefficiency issue. While simple in its form, the introduction of the reference face is very effective and can clearly improve the identity preservation. As a different interpretation of the introduction of the reference face, it is noted that the input faces are noisy (as they are direct estimations during DDPM), which inherently makes the face embedding and the identity loss noisy. In this case, introducing the additional contrastiveness through the reference face can potentially lead to a regularization effect, stabilizing the gradients from the identity loss. The total loss of our model is the L-1 diffusion loss (*aka.* MAE) and the Hard Example Identity Loss with a balancing hyper-parameter w_{HID} :

$$\mathcal{L}_{\text{total}} = \mathcal{L}_{\text{MAE}} + w_{\text{HID}} \cdot \mathcal{L}_{\text{HID}}. \quad (4)$$

3.3 Training-Free Extension for Multi-Reference Faces

Classifier-free guidance [22] is an effective technique for improving diffusion model performance, which is also widely adopted in the image restoration literature [4, 3, 2]. Since our model involves both the LQ condition z_{LQ} and c , we follow [42] for their classifier-free guidance formulation:

$$\tilde{\epsilon}(z_t, z_{\text{LQ}}, c, t) = (1 - s_i)\epsilon(z_t, \emptyset, \emptyset, t) + (s_i - s_c)\epsilon(z_t, z_{\text{LQ}}, \emptyset, t) + s_c\epsilon(z_t, z_{\text{LQ}}, c, t), \quad (5)$$

where s_c controls the guidance effect of the composite context c , and s_i controls the guidance effect of the LQ latent z_{LQ} . The two hyper-parameters s_i and s_c can be adjusted at the inference stage.



Figure 4: Qualitative comparison with other state-of-the-art face restoration methods on FFHQ-Ref Severe [12] test set. The “REF” column is the high-quality reference face image.

While our method is designed to take only one reference face image, it can be extended to support multiple reference faces through a simple ensemble. Let $\mathcal{C} = \{c_i\}_{i=1,\dots,N}$ be a set of composite contexts obtained from N reference face images. The multi-reference inference is formulated as:

$$\tilde{\epsilon}(z_t, z_{LQ}, \mathcal{C}, t) = (1 - s_i)\epsilon(z_t, \emptyset, \emptyset, t) + (s_i - s_c)\epsilon(z_t, z_{LQ}, \emptyset, t) + \frac{s_c}{N} \sum_{i=1}^N \epsilon(z_t, z_{LQ}, c_i, t). \quad (6)$$

Inspired by [12], the identity is expected to be better preserved when more reference faces are provided. Different from [12] which uses multiple reference faces for training, our method only requires one reference face during training while being able to use multiple reference faces during inference. Our method alleviates the data scarcity issue in the multi-reference face scenario, where most training samples only have a single reference face [12]. Such paradigm could be scalable.

4 Experiments

Datasets. Our model is trained on the FFHQ-Ref [12] dataset, which is a subset of FFHQ [43] by person identity clustering. It comprises 18816 images for training and 857 images for testing. We follow [44] for their second-order degradation simulation pipeline during training. For training data augmentation, we use random horizontal flipping with 0.5 probability, and random color jittering with 0.5 probability. For testing purposes, we adopt the identical test data from [12], namely FFHQ-Ref Moderate, FFHQ-Ref Severe, and CelebA-Ref-Test [12]. In this paper, the face image resolution is always 512×512 following previous works [11, 4, 12, 13]. Note, while most previous works do not use identical training data and may potentially suffer from test data leakage [12], our training and test images are completely identical to RefLDM [12] (NeurIPS’24) for a fair comparison.

Implementation Details. We employ an LDM [9] backbone with 865M parameters pre-trained on the WebLI [45] dataset for text-to-image synthesis. We fine-tuned the VAE following [12], using the

Table 1: Comparison with state-of-the-art face restoration methods on FFHQ-Ref Moderate and Severe [12]. The “#REF” means the number of reference face used.

Method	#REF	FFHQ-Ref Moderate							FFHQ-Ref Severe						
		IDS \uparrow	FaceNet \uparrow	IDS(REF) \uparrow	LPIPS \downarrow	MUSIQ \uparrow	NIQE \downarrow	FID \downarrow	IDS \uparrow	FaceNet \uparrow	IDS(REF) \uparrow	LPIPS \downarrow	MUSIQ \uparrow	NIQE \downarrow	FID \downarrow
CodeFormer (NeurIPS’22)	0	0.783	0.822	0.545	0.1839	75.88	4.38	31.7	0.370	0.677	0.265	0.3113	76.12	4.30	49.6
DiffBIR (ECCV’24)	0	<u>0.831</u>	<u>0.842</u>	0.575	0.2268	76.64	5.72	34.9	0.356	0.672	0.253	0.3606	75.71	6.24	55.3
RefLDM (NeurIPS’24)	1	0.826	0.837	0.624	0.2211	72.30	4.61	28.0	0.571	0.733	0.554	0.3366	74.32	4.52	36.0
RestorerID (arXiv)	1	0.804	0.832	0.591	0.2350	73.35	4.98	31.0	0.411	0.690	0.408	0.4130	74.49	4.71	52.7
Ours	1	0.843	0.850	0.732	<u>0.2054</u>	75.29	3.96	25.5	0.609	0.743	0.712	0.3647	75.22	3.84	<u>38.3</u>

Table 2: Multi-reference face inference result on FFHQ-Ref test sets. The identity preservation improves when the number of reference faces increases [12]. Note, the IDS(REF) is calculated using the first reference face, and it may drop with more than one reference face, because the additional reference faces can pull the model output slightly further from the first reference face in Eq. (6).

#REF	FFHQ-Ref Moderate							FFHQ-Ref Severe						
	IDS \uparrow	FaceNet \uparrow	IDS(REF) \uparrow	LPIPS \downarrow	MUSIQ \uparrow	NIQE \downarrow	FID \downarrow	IDS \uparrow	FaceNet \uparrow	IDS(REF) \uparrow	LPIPS \downarrow	MUSIQ \uparrow	NIQE \downarrow	FID \downarrow
1	0.843	0.850	0.732	0.2054	75.29	3.96	25.5	0.609	0.743	0.712	0.3647	75.22	3.84	38.3
2	0.857	0.856	0.693	0.2042	75.28	3.95	25.4	0.640	0.752	0.650	0.3625	75.20	3.82	38.2
3	0.861	0.859	0.683	0.2040	75.29	3.96	25.4	0.652	0.755	0.636	0.3619	75.19	3.82	38.4
4	0.863	0.859	0.680	0.2039	75.29	3.96	25.5	0.657	0.757	0.630	0.3617	75.20	3.82	38.3
5	0.863	0.859	0.678	0.2038	75.29	3.96	25.5	0.658	0.757	0.626	0.3615	75.20	3.83	38.2

68411 remaining FFHQ [43] images after excluding the FFHQ-Ref [12] validation and test images. Our model is trained on the FFHQ-Ref training set for 100K steps, with batch size 256 and learning rate $8e-5$. The cross-attention dimension is 1024. To enable classifier-free guidance [22, 42], we randomly drop the LQ condition as well as the components in Composite Context independently with a 0.1 probability. The Composite Context components are dropped through attention masking. The classifier-guidance scales are selected as $s_i = 1.2$ and $s_c = 1.2$ for inference. The Hard Example Identity Loss balancing parameter w_{HID} is 0.1 following [12], and λ is set as 0.6 by default. The AdaIN [43]-based color fix [2] is applied on the model output as a post-processing step.

Evaluation. Following the previous works [12, 13, 14], we use LPIPS [46] for perceptual similarity, and IDS (*i.e.*, the cosine similarity of ArcFace [16] embedding) for person identity preservation. This “IDS” is calculated between the restoration result and the HQ image. Since we optimize the identity loss using the ArcFace [16] model during training, using IDS alone may not properly reflect generalization performance due to potential overfitting. Thus, we also evaluate the ArcFace IDS with respect to the first reference face for each LQ test image (denoted as “IDS(REF)”), as well as the FaceNet IDS with respect to HQ (denoted as “FaceNet”). We also use no-reference metrics including MUSIQ [47], NIQE [48], and FID [49] for image quality evaluation.

4.1 Experimental Results and Comparison with SOTA

To validate the effectiveness of our proposed method, we evaluate our method on the FFHQ-Ref test datasets with Moderate and Severe degradations, and CelebA-Ref-Test following [12]. We compare our method with some state-of-the-art no-reference face restoration methods, namely CodeFormer [11] and DiffBIR [4], as well as the latest reference-based face restoration methods, namely RefLDM [12] and RestorerID [13]. The quantitative results on FFHQ-Ref test datasets can be found in Table 1. The multi-reference results are in Table 2. The quantitative results on CelebA-Ref-Test can be found in Table 3. The visualization for FFHQ-Ref test sets can be found in Figure 3 and Figure 4. All results of the related works are reproduced using their official code and checkpoints. At the time of writing, some other related works such as OSDFace [18] and InstantRestore [14] have not yet published their code and checkpoints. Hence they are not included for comparison.

As shown in Table 1, the IDS and FaceNet are computed between the output and HQ ground-truth, whereas IDS(REF) is computed between the output and the first reference face. The overall trend is that no-reference methods like CodeFormer [11] and DiffBIR [4] tend to achieve good perceptual similarity (LPIPS) and image quality (MUSIQ), but worse identity preservation compared to reference-based methods like RefLDM [12] and RestorerID [13]. And notably, our model consistently achieves the best identity preservation (which is the top-priority in the reference-based face restoration task) across all test datasets, while still achieving competitive image quality.

Table 4: Ablation study on the Composite Context (CC) and Hard Example Identity Loss (HID).

Modules		FFHQ-Ref Moderate								FFHQ-Ref Severe							
CC	HID	IDS↑	FaceNet↑	IDS(REF)↑	LPIPS↓	MUSIQ↑	NIQE↓	FID↓		IDS↑	FaceNet↑	IDS(REF)↑	LPIPS↓	MUSIQ↑	NIQE↓	FID↓	
-	-	0.811	0.841	0.565	0.2104	76.02	3.85	26.0		0.231	0.637	0.168	0.3896	73.85	3.67	43.4	
✓	-	0.822	0.847	0.584	0.2074	75.66	3.89	25.9		0.345	0.675	0.288	0.3694	75.46	3.83	38.0	
✓	✓	0.843	0.850	0.732	0.2054	75.29	3.96	25.5		0.609	0.743	0.712	0.3647	75.22	3.84	38.3	

Table 5: Ablation study on individual components of Composite Context. The evaluation of different combinations is carried out by using different attention masks with the same model checkpoint.

Composite Context		FFHQ-Ref Moderate								FFHQ-Ref Severe							
High-Level	General	IDS↑	FaceNet↑	IDS(REF)↑	LPIPS↓	MUSIQ↑	NIQE↓	FID↓		IDS↑	FaceNet↑	IDS(REF)↑	LPIPS↓	MUSIQ↑	NIQE↓	FID↓	
-	-	0.738	0.805	0.516	0.2196	74.43	3.99	27.9		0.186	0.616	0.137	0.3875	73.03	3.92	47.4	
-	✓	0.770	0.821	0.567	0.2087	75.01	3.94	25.7		0.348	0.666	0.320	0.3713	74.51	3.83	40.1	
✓	-	0.835	0.846	0.707	0.2094	75.20	3.98	25.9		0.535	0.717	0.625	0.3800	74.95	3.85	40.2	
✓	✓	0.843	0.850	0.732	0.2054	75.29	3.96	25.5		0.609	0.743	0.712	0.3647	75.22	3.84	38.3	

As shown in Table 2, the identity preservation will improve as we introduce more reference faces. The effect saturates at roughly five images, which is similar to the observation in [12]. Note, the IDS(REF) is calculated using the first available reference face. That means the additional reference faces could pull the model output slightly further from the first reference through Eq. (6). Thus, IDS(REF) may drop with additional reference faces. Nevertheless, our worst IDS(REF) is still higher than previous methods in Table 1.

As shown in Figure 3 for FFHQ-Ref Moderate, when the input LQ image contains a moderate degradation, the IDS performance gap among the models is not very large in Table 1, hence it is highly recommended to zoom-in to visually distinguish the differences in restored face details. For instance, the black moles are well preserved on the sixth row in Figure 3. While other methods tends to excessively smooth the skin texture, our model generates more realistic textures.

As shown in Figure 4 for FFHQ-Ref Severe, when the LQ face is almost unrecognizable, our method can still sufficiently leverage the reference face and generate a face that is very close to the ground truth, preserving identity. In contrast, almost every other method generates a visually different person in most cases, which justifies the consistent improvements on the identity metrics of our method.

As demonstrated in Table 3 for CelebA-Ref-Test, our model still achieves the best identity preservation compared to other reference-based methods. All the above experimental results demonstrate the effectiveness of our method, especially in terms of identity preservation.

Table 3: Comparison with the state-of-the-art reference-based methods on the CelebA-Ref-Test [12] dataset.

Method	#REF	CelebA-Ref-Test					
		IDS↑	FaceNet↑	IDS(REF)↑	LPIPS↓	MUSIQ↑	NIQE↓
RefLDM	1	0.768	0.821	0.564	0.2453	72.11	4.75
RestorerID	1	0.756	0.820	0.527	0.2690	74.86	5.22
Ours	1	0.779	0.827	0.691	0.2310	75.64	3.98

4.2 Ablation Study and Discussions

We conduct the ablation study in a hierarchical way, firstly, coarse-grained based on the two Composite Context and Hard Example Identity Loss modules. Then we conduct the fine-grained ablation study for each component in these modules.

Module-wise Ablation. Since the two modules are independent of each other, we conduct the ablation study by removing some of them, and then retrain the model. As shown in Table 4, both the context and loss contribute significantly to the final performance, because the removal of any of them will lead to a major performance drop. Removing both makes the model degenerate into a no-reference face restoration model, which lags behind our model too much in identity preservation. This means both Composite Context and Hard Example Identity Loss are effective. Next, we conduct an ablation study on the individual components of these modules.

Composite Context Ablation. As shown in Table 5, we study the contribution of individual components in the Composite Context by applying attention masks during inference. It can be seen in the table that all the multi-level components, including high-level and general components clearly contribute significantly to the final performance, as the removal of any of them will lead to a performance drop, especially on the FFHQ-Ref Severe test dataset.

Table 6: Ablation Study on Individual Components of the Hard Identity Loss.

λ	FFHQ-Ref Moderate							FFHQ-Ref Severe						
	IDS \uparrow	FaceNet \uparrow	IDS(REF) \uparrow	LPIPS \downarrow	MUSIQ \uparrow	NIQE \downarrow	FID \downarrow	IDS \uparrow	FaceNet \uparrow	IDS(REF) \uparrow	LPIPS \downarrow	MUSIQ \uparrow	NIQE \downarrow	FID \downarrow
0	0.844	0.855	0.621	0.2039	75.36	3.97	25.5	0.485	0.712	0.465	0.3664	75.22	3.85	38.5
0.6	0.843	0.850	0.732	0.2054	75.29	3.96	25.5	0.609	0.743	0.712	0.3647	75.22	3.84	38.3
1	0.779	0.821	0.794	0.2076	75.43	3.95	25.6	0.605	0.742	0.768	0.3666	75.29	3.90	38.8

Hard Example Identity Loss Ablation. As shown in Table 6, we conduct an ablation study on the individual components in the Hard Example Identity Loss, by adjusting the balancing parameter λ between the HQ image and the reference image in Eq. (3). According to the results, when we only use the ID loss with the HQ image ($\lambda = 0$), the IDS(REF) is much lower, so is IDS on FFHQ-Ref Severe. When we only use the ID loss with the REF image ($\lambda = 1$), the IDS will be traded off with IDS(REF). Hence, we empirically set the λ parameter as 0.6 by default, by considering all the three identity preservation metrics. The case where the Hard Identity Loss is removed ($w_{\text{HID}} = 0$) is at the second row of Table 4, and that leads to a much lower performance regardless of the λ parameter.

Influence of Reference Face. The above ablation study supports the effectiveness of our method when using the a *correct* reference face. While the problem of reference-based face restoration assumes a reference face with correct identity is provided, it is difficult to guarantee in real-world applications. To demonstrate the influence of the reference face, we deliberately use a *wrong* reference face, as shown in Figure 5. According to our observation, when the input LQ image has moderate information loss with the person identity roughly recognizable, our model will largely follow the LQ, and add slight identity-related details to the result, as shown in the first row in the figure. When the input LQ has severe information loss with the person identity almost unrecognizable, the REF face image becomes dominant and show stronger impact in the resulting image.

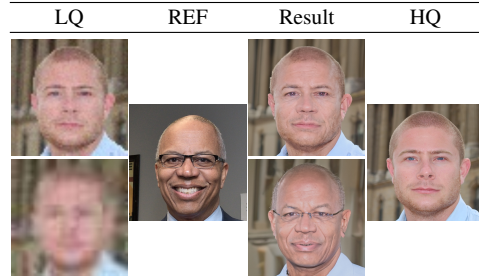


Figure 5: Demonstration of the impact of reference face image, by deliberately supplying the model with a reference face of a wrong identity. The first row is from FFHQ-Ref Moderate, and the second row is from FFHQ-Ref Severe.

This phenomenon, on the one hand, further demonstrates the effectiveness of our method through the influence of the reference face. On the other hand, it also implies the importance of ensuring the correct identity in real-world applications for reference-based face restoration.

Limitations and Future Work. (1) The face restoration model is trained on simulated degradation pipelines [44], which means it may underperform on in-the-wild face images with unknown degradations. (2) While the reference-based face restoration task assume high-quality reference images are available, in practical scenarios the reference image quality may vary. In that case, exploring different weighting mechanisms in Eq. (6) could be a potential direction for future exploration. (3) A large-scale high-quality dataset for reference-based face restoration is still missing, and the FFHQ-Ref [12] training set only contains 18816 images. One potential approach to obtain more data could be filtering face recognition datasets [50]. We leave these directions for future study.

Broader Impact. Our method aims at restoring low-quality face images, with the goal of contributing positively to society. However, being a diffusion-based face generative model, it might be abused to forge DeepFake [51] images. We suggest real-world face restoration service providers apply invisible watermarks [52] to the generated result to mitigate potential risks and negative societal impact.

5 Conclusion

We present a reference-based face restoration method, highlighting two key modules: Composite Context and Hard Example Identity Loss that focus on identity preservation. The two key modules are designed to better exploit reference face images, while all the existing works leverage it to a lesser extent. Meanwhile, the proposed method can be extended for the multi-reference case in a training-free manner. Experimental results on the FFHQ-Ref and CelebA-Ref-Test datasets demonstrate the effectiveness of our proposed method. Ablation studies on the Composite Context and Hard

Example Identity Loss suggest that all the proposed modules in our method, including the individual components in the modules, are effective and make a considerable impact on identity preservation.

Acknowledgement. We are grateful to Mojtaba Ardakani for his assistance with the diffusion formulation and code review, to Julian Iseringhausen for his help in fine-tuning the VAE on face images, and to Xiang Zhu for insightful discussions.

References

- [1] Xintao Wang, Ke Yu, Shixiang Wu, Jinjin Gu, Yihao Liu, Chao Dong, Chen Change Loy, Yu Qiao, and Xiaoou Tang. Esrgan: Enhanced super-resolution generative adversarial networks, 2018.
- [2] Jianyi Wang, Zongsheng Yue, Shangchen Zhou, Kelvin C.K. Chan, and Chen Change Loy. Exploiting diffusion prior for real-world image super-resolution. 2024.
- [3] Fanghua Yu, Jinjin Gu, Zheyuan Li, Jinfan Hu, Xiangtao Kong, Xintao Wang, Jingwen He, Yu Qiao, and Chao Dong. Scaling up to excellence: Practicing model scaling for photo-realistic image restoration in the wild, 2024.
- [4] Xinqi Lin, Jingwen He, Ziyang Chen, Zhaoyang Lyu, Bo Dai, Fanghua Yu, Wanli Ouyang, Yu Qiao, and Chao Dong. Diffbir: Towards blind image restoration with generative diffusion prior, 2024.
- [5] Rongyuan Wu, Tao Yang, Lingchen Sun, Zhengqiang Zhang, Shuai Li, and Lei Zhang. Seesr: Towards semantics-aware real-world image super-resolution. In *Proceedings of the IEEE/CVF conference on computer vision and pattern recognition*, pages 25456–25467, 2024.
- [6] Tao Yang, Rongyuan Wu, Peiran Ren, Xuansong Xie, , and Lei Zhang. Pixel-aware stable diffusion for realistic image super-resolution and personalized stylization. In *The European Conference on Computer Vision (ECCV) 2024*, 2023.
- [7] Jonathan Ho, Ajay Jain, and Pieter Abbeel. Denoising diffusion probabilistic models, 2020.
- [8] Jiaming Song, Chenlin Meng, and Stefano Ermon. Denoising diffusion implicit models, 2022.
- [9] Robin Rombach, Andreas Blattmann, Dominik Lorenz, Patrick Esser, and Björn Ommer. High-resolution image synthesis with latent diffusion models, 2022.
- [10] Dustin Podell, Zion English, Kyle Lacey, Andreas Blattmann, Tim Dockhorn, Jonas Müller, Joe Penna, and Robin Rombach. Sdxl: Improving latent diffusion models for high-resolution image synthesis, 2023.
- [11] Shangchen Zhou, Kelvin C.K. Chan, Chongyi Li, and Chen Change Loy. Towards robust blind face restoration with codebook lookup transformer. In *NeurIPS*, 2022.
- [12] Chi-Wei Hsiao, Yu-Lun Liu, Cheng-Kun Yang, Sheng-Po Kuo, Yuchun Kevin Jou, and Chia-Ping Chen. Ref-ldm: A latent diffusion model for reference-based face image restoration. In *Advances in Neural Information Processing Systems*, 2024.
- [13] Jiacheng Ying, Mushui Liu, Zhe Wu, Runming Zhang, Zhu Yu, Siming Fu, Si-Yuan Cao, Chao Wu, Yunlong Yu, and Hui-Liang Shen. Restorerid: Towards tuning-free face restoration with id preservation, 2024.
- [14] Howard Zhang, Yuval Alaluf, Sizhuo Ma, Achuta Kadambi, Jian Wang, and Kfir Aberman. Instantrestore: Single-step personalized face restoration with shared-image attention, 2024.
- [15] Xiaoming Li, Shiguang Zhang, Shangchen Zhou, Lei Zhang, and Wangmeng Zuo. Learning dual memory dictionaries for blind face restoration, 2022.
- [16] Jiankang Deng, Jia Guo, Jing Yang, Niannan Xue, Irene Kotsia, and Stefanos Zafeiriou. Arcface: Additive angular margin loss for deep face recognition. *IEEE Transactions on Pattern Analysis and Machine Intelligence*, 44(10):5962–5979, October 2022.
- [17] Yinglin Zheng, Hao Yang, Ting Zhang, Jianmin Bao, Dongdong Chen, Yangyu Huang, Lu Yuan, Dong Chen, Ming Zeng, and Fang Wen. General facial representation learning in a visual-linguistic manner. *arXiv preprint arXiv:2112.03109*, 2021.
- [18] Jingkai Wang, Jue Gong, Lin Zhang, Zheng Chen, Xing Liu, Hong Gu, Yutong Liu, Yulun Zhang, and Xiaokang Yang. Osdface: One-step diffusion model for face restoration, 2025.

- [19] Florian Schroff, Dmitry Kalenichenko, and James Philbin. Facenet: A unified embedding for face recognition and clustering. In *2015 IEEE Conference on Computer Vision and Pattern Recognition (CVPR)*, page 815–823. IEEE, June 2015.
- [20] Kevin Musgrave, Serge Belongie, and Ser-Nam Lim. A metric learning reality check, 2020.
- [21] Karsten Roth, Timo Milbich, Samarth Sinha, Prateek Gupta, Björn Ommer, and Joseph Paul Cohen. Revisiting training strategies and generalization performance in deep metric learning, 2020.
- [22] Jonathan Ho and Tim Salimans. Classifier-free diffusion guidance, 2022.
- [23] Yang Song, Prafulla Dhariwal, Mark Chen, and Ilya Sutskever. Consistency models, 2023.
- [24] Prafulla Dhariwal and Alex Nichol. Diffusion models beat gans on image synthesis, 2021.
- [25] Yang Song, Jascha Sohl-Dickstein, Diederik P. Kingma, Abhishek Kumar, Stefano Ermon, and Ben Poole. Score-based generative modeling through stochastic differential equations, 2021.
- [26] Kangfu Mei, Hossein Talebi, Mojtaba Ardakani, Vishal M Patel, Peyman Milanfar, and Mauricio Delbracio. The power of context: How multimodality improves image super-resolution. In *Proceedings of the IEEE/CVF Conference on Computer Vision and Pattern Recognition*, 2025.
- [27] Yu Chen, Ying Tai, Xiaoming Liu, Chunhua Shen, and Jian Yang. Fsrnet: End-to-end learning face super-resolution with facial priors, 2017.
- [28] Xiaoming Li, Wenyu Li, Dongwei Ren, Hongzhi Zhang, Meng Wang, and Wangmeng Zuo. Enhanced blind face restoration with multi-exemplar images and adaptive spatial feature fusion. In *CVPR*, 2020.
- [29] Xintao Wang, Yu Li, Honglun Zhang, and Ying Shan. Towards real-world blind face restoration with generative facial prior, 2021.
- [30] Peiqing Yang, Shangchen Zhou, Qingyi Tao, and Chen Change Loy. PGDiff: Guiding diffusion models for versatile face restoration via partial guidance. In *NeurIPS*, 2023.
- [31] Xiaoming Li, Chaofeng Chen, Shangchen Zhou, Xianhui Lin, Wangmeng Zuo, and Lei Zhang. Blind face restoration via deep multi-scale component dictionaries. In *ECCV*, 2020.
- [32] Ashish Vaswani, Noam Shazeer, Niki Parmar, Jakob Uszkoreit, Llion Jones, Aidan N. Gomez, Lukasz Kaiser, and Illia Polosukhin. Attention is all you need, 2023.
- [33] Geon Min, Tae Bok Lee, and Yong Seok Heo. Pdgrad: Guiding diffusion model for reference-based blind face restoration with pivot direction gradient guidance. *Sensors*, 24(22), 2024.
- [34] Tuomas Varanka, Tapani Toivonen, Soumya Tripathy, Guoying Zhao, and Erman Acar. Pfstorer: Personalized face restoration and super-resolution, 2024.
- [35] Siyu Liu, Zheng-Peng Duan, Jia OuYang, Jiayi Fu, Hyunhee Park, Zikun Liu, Chun-Le Guo, and Chongyi Li. Faceme: Robust blind face restoration with personal identification, 2025.
- [36] Chenyang Wang, Wenjie An, Kui Jiang, Xianming Liu, and Junjun Jiang. Llv-fsr: Exploiting large language-vision prior for face super-resolution, 2024.
- [37] Olaf Ronneberger, Philipp Fischer, and Thomas Brox. U-net: Convolutional networks for biomedical image segmentation, 2015.
- [38] Kaiming He, Xiangyu Zhang, Shaoqing Ren, and Jian Sun. Deep residual learning for image recognition, 2015.
- [39] Alexey Dosovitskiy, Lucas Beyer, Alexander Kolesnikov, Dirk Weissenborn, Xiaohua Zhai, Thomas Unterthiner, Mostafa Dehghani, Matthias Minderer, Georg Heigold, Sylvain Gelly, Jakob Uszkoreit, and Neil Houlsby. An image is worth 16x16 words: Transformers for image recognition at scale, 2021.
- [40] Mo Zhou and Vishal M. Patel. Enhancing adversarial robustness for deep metric learning, 2022.
- [41] Mo Zhou, Le Wang, Zhenxing Niu, Qilin Zhang, Nanning Zheng, and Gang Hua. Adversarial attack and defense in deep ranking. *IEEE Transactions on Pattern Analysis and Machine Intelligence*, 46(8):5306–5324, 2024.
- [42] Tim Brooks, Aleksander Holynski, and Alexei A. Efros. Instructpix2pix: Learning to follow image editing instructions, 2023.

- [43] Tero Karras, Samuli Laine, and Timo Aila. A style-based generator architecture for generative adversarial networks, 2019.
- [44] Xintao Wang, Liangbin Xie, Chao Dong, and Ying Shan. Real-esrgan: Training real-world blind super-resolution with pure synthetic data, 2021.
- [45] Xi Chen, Xiao Wang, Soravit Changpinyo, AJ Piergiovanni, Piotr Padlewski, Daniel Salz, Sebastian Goodman, Adam Grycner, Basil Mustafa, Lucas Beyer, Alexander Kolesnikov, Joan Puigcerver, Nan Ding, Keran Rong, Hassan Akbari, Gaurav Mishra, Linting Xue, Ashish Thapliyal, James Bradbury, Weicheng Kuo, Mojtaba Seyedhosseini, Chao Jia, Burcu Karagol Ayan, Carlos Riquelme, Andreas Steiner, Anelia Angelova, Xiaohua Zhai, Neil Houlsby, and Radu Soricut. Pali: A jointly-scaled multilingual language-image model, 2023.
- [46] Richard Zhang, Phillip Isola, Alexei A. Efros, Eli Shechtman, and Oliver Wang. The unreasonable effectiveness of deep features as a perceptual metric, 2018.
- [47] Junjie Ke, Qifei Wang, Yilin Wang, Peyman Milanfar, and Feng Yang. Musiq: Multi-scale image quality transformer, 2021.
- [48] Anish Mittal, Rajiv Soundararajan, and Alan C Bovik. Making a “completely blind” image quality analyzer. *IEEE Signal processing letters*, 20(3):209–212, 2012.
- [49] Martin Heusel, Hubert Ramsauer, Thomas Unterthiner, Bernhard Nessler, and Sepp Hochreiter. Gans trained by a two time-scale update rule converge to a local nash equilibrium, 2018.
- [50] Zheng Zhu, Guan Huang, Jiankang Deng, Yun Ye, Junjie Huang, Xinze Chen, Jiagang Zhu, Tian Yang, Jiwen Lu, Dalong Du, and Jie Zhou. Webface260m: A benchmark unveiling the power of million-scale deep face recognition, 2021.
- [51] Gan Pei, Jiangning Zhang, Menghan Hu, Zhenyu Zhang, Chengjie Wang, Yunsheng Wu, Guangtao Zhai, Jian Yang, Chunhua Shen, and Dacheng Tao. Deepfake generation and detection: A benchmark and survey, 2024.
- [52] Pierre Fernandez, Hady Elsahar, I. Zeki Yalniz, and Alexandre Mourachko. Video seal: Open and efficient video watermarking. *arXiv preprint arXiv:2412.09492*, 2024.

A Detailed Quantitative Results and More Visualizations

The detailed results and comparison with state-of-the-art methods on FFHQ-Ref Moderate, FFHQ-Ref Severe, and CelebA-Ref-Test can be found in Table 7, Table 8, and Table 9, respectively. Additional visualizations are provided in Figure 6, Figure 7, and Figure 8 for those three test sets.

The detailed multi-reference face restoration results and comparison with state-of-the-art methods can be found in Table 10, Table 11, and Table 12, respectively for the three test sets. Some visualizations are provided in Figure 9 to demonstrate the effect of using more than one reference faces.

Additional visualizations with wrong reference face (as discussed in Section 4.2) can be found in Figure 10, Figure 11, and Figure 12. A minor ablation study on the classifier-free guidance scale parameter can be found in Table 13.

Table 7: Detailed Quantitative Results on FFHQ-Ref Moderate test set.

Method	#REF	FFHQ-Ref Moderate						
		IDS	FaceNet	IDS(REF)	LPIPS	MUSIQ	NIQE	FID
CodeFormer	0	0.783 \pm 0.082	0.822 \pm 0.047	0.545 \pm 0.106	0.1839 \pm 0.0471	75.88 \pm 2.01	4.38 \pm 0.69	31.7
DiffBIR	0	0.831 \pm 0.095	0.842 \pm 0.056	0.575 \pm 0.108	0.2268 \pm 0.0633	76.64 \pm 1.64	5.72 \pm 1.23	34.9
RefLDM	1	0.826 \pm 0.077	0.837 \pm 0.048	0.624 \pm 0.096	0.2210 \pm 0.0583	72.30 \pm 4.89	4.61 \pm 0.64	28.0
RestorerID	1	0.804 \pm 0.099	0.832 \pm 0.054	0.591 \pm 0.096	0.2350 \pm 0.0688	73.35 \pm 5.12	4.98 \pm 0.81	31.0
Ours	1	0.843 \pm 0.076	0.850 \pm 0.051	0.732 \pm 0.069	0.2054 \pm 0.0606	75.29 \pm 2.77	3.96 \pm 0.71	25.5

Table 8: Detailed Quantitative Results on FFHQ-Ref Severe test set.

Method	#REF	FFHQ-Ref Severe						
		IDS	FaceNet	IDS(REF)	LPIPS	MUSIQ	NIQE	FID
CodeFormer	0	0.370 ± 0.150	0.677 ± 0.061	0.265 ± 0.132	0.3113 ± 0.0801	76.12 ± 1.94	4.30 ± 0.70	49.6
DiffBIR	0	0.356 ± 0.144	0.672 ± 0.058	0.253 ± 0.124	0.3606 ± 0.0879	75.71 ± 2.81	6.24 ± 1.22	55.3
RefLDM	1	0.571 ± 0.110	0.733 ± 0.052	0.554 ± 0.112	0.3366 ± 0.0756	74.32 ± 3.36	4.52 ± 0.62	36.0
RestorerID	1	0.411 ± 0.110	0.690 ± 0.052	0.408 ± 0.103	0.4130 ± 0.0741	74.49 ± 3.41	4.71 ± 0.65	52.7
Ours	1	0.609 ± 0.089	0.743 ± 0.048	0.712 ± 0.068	0.3647 ± 0.0722	75.22 ± 2.46	3.84 ± 0.64	38.3

Table 9: Detailed Quantitative Results on CelebA-Ref-Test test set.

Method	#REF	CelebA-Ref-Test						
		IDS	FaceNet	IDS(REF)	LPIPS	MUSIQ	NIQE	FID
RefLDM	1	0.768 ± 0.085	0.821 ± 0.046	0.564 ± 0.096	0.2453 ± 0.0550	72.11 ± 4.59	4.75 ± 0.55	19.4
RestorerID	1	0.756 ± 0.098	0.820 ± 0.049	0.527 ± 0.090	0.2690 ± 0.0629	74.86 ± 3.82	5.22 ± 0.76	25.4
Ours	1	0.779 ± 0.086	0.827 ± 0.048	0.691 ± 0.064	0.2310 ± 0.0540	75.64 ± 2.44	3.98 ± 0.53	18.4

Table 10: Detailed Quantitative Results on FFHQ-Ref Moderate test set. Note, our multi-reference face support is training-free, while RefLDM's is not.

Method	#REF	FFHQ-Ref Moderate						
		IDS	FaceNet	IDS(REF)	LPIPS	MUSIQ	NIQE	FID
RefLDM	1	0.826 ± 0.077	0.837 ± 0.048	0.624 ± 0.096	0.2210 ± 0.0583	72.30 ± 4.89	4.61 ± 0.64	28.0
Ours	1	0.843 ± 0.076	0.850 ± 0.051	0.732 ± 0.069	0.2054 ± 0.0606	75.29 ± 2.77	3.96 ± 0.71	25.5
RefLDM	2	0.839 ± 0.067	0.844 ± 0.045	0.630 ± 0.094	0.2150 ± 0.0577	73.25 ± 4.34	4.57 ± 0.62	27.6
Ours	2	0.857 ± 0.069	0.856 ± 0.049	0.693 ± 0.075	0.2042 ± 0.0603	75.28 ± 2.75	3.95 ± 0.71	25.4
RefLDM	3	0.845 ± 0.063	0.847 ± 0.045	0.635 ± 0.092	0.2117 ± 0.0574	73.87 ± 3.92	4.53 ± 0.63	27.2
Ours	3	0.861 ± 0.067	0.859 ± 0.049	0.683 ± 0.077	0.2040 ± 0.0602	75.29 ± 2.75	3.96 ± 0.71	25.5
RefLDM	4	0.848 ± 0.061	0.848 ± 0.044	0.639 ± 0.090	0.2101 ± 0.0573	74.26 ± 3.66	4.50 ± 0.63	27.2
Ours	4	0.863 ± 0.066	0.859 ± 0.049	0.680 ± 0.078	0.2039 ± 0.0602	75.29 ± 2.75	3.96 ± 0.71	25.5
RefLDM	5	0.848 ± 0.060	0.848 ± 0.043	0.641 ± 0.090	0.2097 ± 0.0574	74.51 ± 3.52	4.48 ± 0.64	27.1
Ours	5	0.863 ± 0.066	0.859 ± 0.048	0.678 ± 0.079	0.2038 ± 0.0601	75.29 ± 2.75	3.96 ± 0.71	25.5

Table 11: Detailed Quantitative Results on FFHQ-Ref Severe test set. Note, our multi-reference face support is training-free, while RefLDM's is not.

Method	#REF	FFHQ-Ref Severe						
		IDS	FaceNet	IDS(REF)	LPIPS	MUSIQ	NIQE	FID
RefLDM	1	0.571 ± 0.110	0.733 ± 0.052	0.554 ± 0.112	0.3366 ± 0.0756	74.32 ± 3.36	4.52 ± 0.62	36.0
Ours	1	0.609 ± 0.089	0.743 ± 0.048	0.712 ± 0.068	0.3647 ± 0.0722	75.22 ± 2.46	3.84 ± 0.64	38.3
RefLDM	2	0.631 ± 0.091	0.754 ± 0.049	0.576 ± 0.100	0.3271 ± 0.0745	74.82 ± 3.20	4.51 ± 0.62	35.4
Ours	2	0.640 ± 0.078	0.752 ± 0.047	0.650 ± 0.073	0.3625 ± 0.0717	75.20 ± 2.42	3.82 ± 0.63	38.2
RefLDM	3	0.662 ± 0.084	0.764 ± 0.047	0.594 ± 0.095	0.3228 ± 0.0740	75.22 ± 2.90	4.49 ± 0.64	35.1
Ours	3	0.652 ± 0.075	0.755 ± 0.047	0.636 ± 0.074	0.3619 ± 0.0715	75.19 ± 2.46	3.82 ± 0.63	38.4
RefLDM	4	0.677 ± 0.080	0.769 ± 0.047	0.604 ± 0.093	0.3203 ± 0.0731	75.46 ± 2.73	4.46 ± 0.64	34.7
Ours	4	0.657 ± 0.074	0.757 ± 0.048	0.630 ± 0.075	0.3617 ± 0.0715	75.20 ± 2.42	3.82 ± 0.63	38.3
RefLDM	5	0.685 ± 0.078	0.772 ± 0.048	0.611 ± 0.091	0.3201 ± 0.0733	75.62 ± 2.68	4.46 ± 0.66	34.7
Ours	5	0.658 ± 0.074	0.757 ± 0.049	0.626 ± 0.077	0.3615 ± 0.0714	75.20 ± 2.42	3.83 ± 0.63	38.2

Table 12: Detailed Quantitative Results on CelebA-Ref-Test test set. Note, our multi-reference face support is training-free, while RefLDM’s is not.

Method	#REF	CelebA-Ref-Test						
		IDS	FaceNet	IDS(REF)	LPIPS	MUSIQ	NIQE	FID
RefLDM	1	0.768 ± 0.085	0.821 ± 0.046	0.564 ± 0.096	0.2453 ± 0.0550	72.11 ± 4.59	4.75 ± 0.55	19.4
Ours	1	0.779 ± 0.086	0.827 ± 0.048	0.691 ± 0.064	0.2310 ± 0.0540	75.64 ± 2.44	3.98 ± 0.53	18.4
RefLDM	2	0.775 ± 0.081	0.824 ± 0.045	0.580 ± 0.095	0.2428 ± 0.0545	73.01 ± 4.18	4.69 ± 0.57	18.8
Ours	2	0.787 ± 0.084	0.831 ± 0.047	0.675 ± 0.071	0.2305 ± 0.0540	75.65 ± 2.43	3.98 ± 0.53	18.4
RefLDM	3	0.774 ± 0.080	0.824 ± 0.044	0.587 ± 0.095	0.2426 ± 0.0542	73.46 ± 4.02	4.63 ± 0.56	18.4
Ours	3	0.787 ± 0.084	0.831 ± 0.047	0.668 ± 0.076	0.2305 ± 0.0540	75.65 ± 2.43	3.98 ± 0.53	18.4
RefLDM	4	0.771 ± 0.080	0.824 ± 0.044	0.591 ± 0.095	0.2434 ± 0.0542	73.73 ± 3.93	4.59 ± 0.57	18.1
Ours	4	0.786 ± 0.084	0.831 ± 0.047	0.664 ± 0.080	0.2305 ± 0.0540	75.65 ± 2.43	3.98 ± 0.53	18.4
RefLDM	5	0.767 ± 0.081	0.822 ± 0.045	0.594 ± 0.096	0.2445 ± 0.0542	73.93 ± 3.88	4.56 ± 0.57	18.0
Ours	5	0.785 ± 0.085	0.830 ± 0.046	0.661 ± 0.082	0.2306 ± 0.0540	75.65 ± 2.43	3.98 ± 0.53	18.4

Table 13: Ablation study on the classifier-free guidance scale parameters with FFHQ-Ref Severe.

s_i	s_c	FFHQ-Ref Severe						
		IDS	FaceNet	IDS(REF)	LPIPS	MUSIQ	NIQE	FID
1.0	1.0	0.599 ± 0.089	0.738 ± 0.049	0.694 ± 0.070	0.3645 ± 0.0723	74.73 ± 2.73	3.97 ± 0.61	39.1
1.0	1.2	0.608 ± 0.088	0.742 ± 0.048	0.719 ± 0.065	0.3678 ± 0.0723	75.13 ± 2.57	3.94 ± 0.63	38.8
1.2	1.0	0.598 ± 0.091	0.738 ± 0.050	0.685 ± 0.073	0.3642 ± 0.0724	74.84 ± 2.65	3.85 ± 0.63	38.8
1.2	1.2	0.609 ± 0.089	0.743 ± 0.048	0.712 ± 0.068	0.3647 ± 0.0722	75.22 ± 2.46	3.84 ± 0.64	38.3



Figure 6: Additional qualitative comparison with other state-of-the-art face restoration methods on FFHQ-Ref Moderate test set. The “REF” column is the high-quality reference face image.



Figure 7: Additional qualitative comparison with other state-of-the-art face restoration methods on FFHQ-Ref Severe test set. The “REF” column is the high-quality reference face image.



Figure 8: Additional qualitative comparison with other state-of-the-art face restoration methods on CelebA-Ref-Test test set. The “REF” column is the high-quality reference face image.

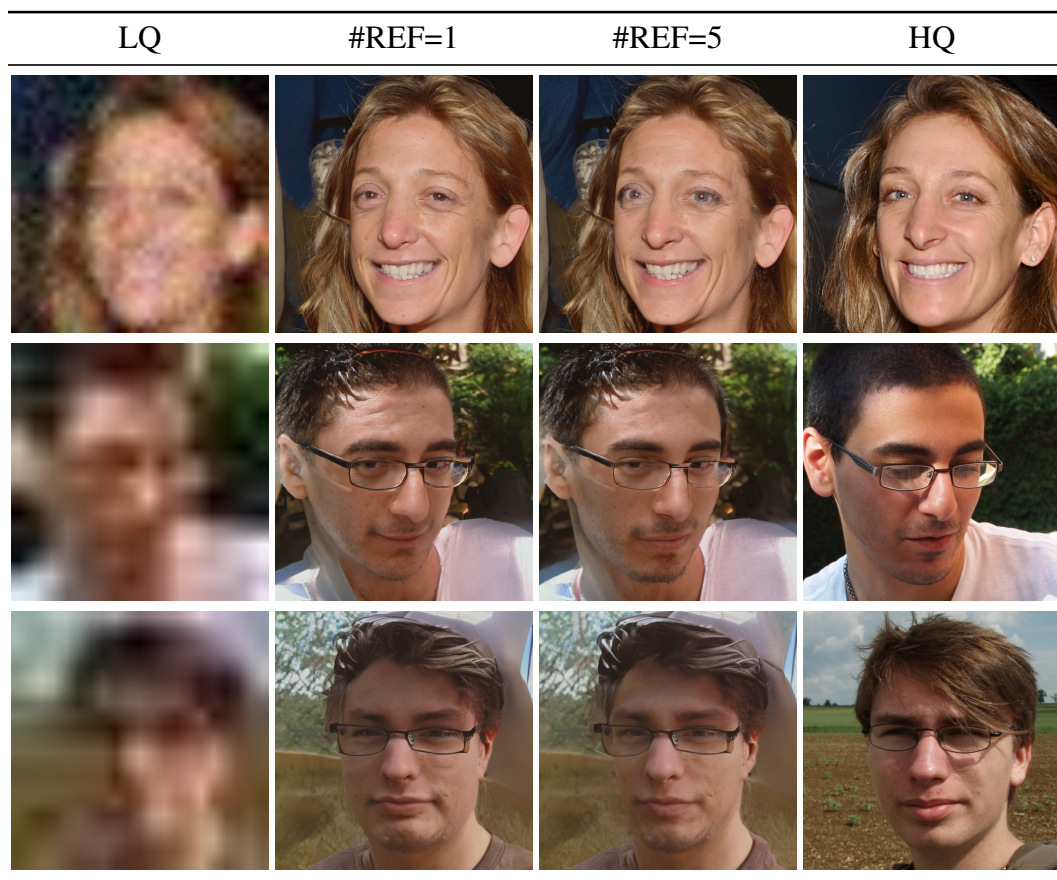


Figure 9: Visualization of multi-reference face restoration on FFHQ-Ref Severe.

LQ	REF	Result	HQ
			
			
			
			

Figure 10: Additional visualizations with wrong reference face. This table is a continuation of the Figure 5 in the manuscript. As discussed in the manuscript, a wrong reference face will leads to some “identity blending” effect depending on how much information is lost from the low-quality input face.

LQ	REF	Result	HQ
			
			
			
			

Figure 11: Additional visualizations with wrong reference face. This table is a continuation of the Figure 5 in the manuscript. As discussed in the manuscript, a wrong reference face will leads to some “identity blending” effect depending on how much information is lost from the low-quality input face.

















LQ	REF	Result	HQ
			
			
			
			

Figure 12: Additional visualizations with wrong reference face. This table is a continuation of the Figure 5 in the manuscript. As discussed in the manuscript, a wrong reference face will leads to some “identity blending” effect depending on how much information is lost from the low-quality input face.